South African Journal of Chemical Engineering 35 (2021) 159–164

Contents lists available at ScienceDirect

South African Journal of Chemical Engineering

journal homepage: www.elsevier.com/locate/sajce

Editorial

Corrosion inhibition effect of citrus sinensis essential oil extract on plain carbon steel in dilute acid media

Roland Tolulope Loto*, Ekene Henry Mbah, Jennifer Iruoma Ugada

Department of Mechanical Engineering, Covenant University, Ota, Ogun State, Nigeria

ARTICLE INFO

Keywords:
Corrosion
Adsorption
Carbon steel
Inhibitor

ABSTRACT

The inhibition performance of essential oil extracts of citrus sinensis (CS) on the corrosion of plain carbon steel (PCS) in 0.5 M H_2SO_4 and 0.5 M HCl solution was evaluated by weight loss measurement, potentiodynamic polarization technique, optical macroscopy and ATF-FTIR spectroscopy. CS more effectively inhibited PCS corrosion in HCl solution compared to H_2SO_4 with optimal inhibition result of 81.61% in HCl and 76.95% in H_2SO_4 from weight loss measurement. The corresponding values from potentiodynamic polarization are 94.90% in HCl and 76.93% in H_2SO_4 solutions respectively. Inhibition efficiency generally decreased with respect to exposure time, but increased with increase in inhibitor concentration in both acids. The inhibition performance of CS was observed to be mixed type inhibition effect in both acids with dominant cathodic inhibition reaction mechanism at 6%-10% CS concentration in HCl solution. CS influenced the anodic cathodic polarization plots in H_2SO_4 solution through surface coverage of the steel inhibiting the redox electrochemical process. In HCl significant influence of the anodic-cathodic polarization plots results in pseudo passivation behavior during potential scanning. Inhibition. FTIR spectra peaks showed aggregation of CS molecular functional groups with decreased transmittance over a wide spectrum in corroded H_2SO_4 solution compared to specific spectra peaks in HCl with decreased transmittance due to limited absorption of protonated CS molecules. Optical images of corroded and non-inhibited PCS specimen from both acids exhibited severe surface degradation with macro pits visible on the steel from H_2SO_4 solution. The inhibited steel from both acids displayed improved surface morphology due to surface protection effect of CS molecules.

1. Introduction

Carbon steels corrosion has been a significant issue globally attracting the attention of scientific for cost effective solution (Liu et al., 2001; Collins et al., 1993; Ekpe et al., 1995). The issue stems from the extensive industrial application of the steel in petrochemical, oil refinery, building and construction, chemical processing, energy generation, automobile, marine and mining industries. During application the steel exhibits weak resistance to corrosion due to its inability to passivation in corrosive environments. The oxide which forms on the steel is porous allowing the corrosion process to continue on the substrate Fe. As a result, enormous damages do occur leading to high cost of maintenance, repair and corrosion (Ashassi-Sorkhabi et al., 2009; Singh et al., 1995; Ahmad, 2006). Anions of sulphates, nitrates, chlorides, thiosulphates etc. encountered in industry are responsible for the corrosion damage on carbon steels significantly decreasing their operational lifespan. Chemical compounds known as corrosion inhibitors are the most cost effective alternative for suppressing the corrosion damage on carbon steels (Ahmad, 2006). Inhibitors commonly in application today are of organic origin which adsorbs onto the steel surface (Dariva and Alexandre, 2014; Kuznetsov,1996; Loto and Loto, 2012; Rivera-Grau et al., 2013; Winkler, 2017; Loto and Loto, 2013). However, most organic compounds are toxic, unsustainable, and costly. Research on green chemical compounds for corrosion inhibition of carbon steels is on-going. Most green chemical compounds perform poorly and being highly biodegradable; expires over a short time and lack strong adsorption properties on mild steel (Loto et al., 2018; Loto, 2017 l; Ramezanzadeh et al., 2018; Bahlakeh et al., 2017; Dehghani et al., 2020). Essential oil extracts have been proven to be effective but their performance so far is highly concentration dependent but yet promising (Dehghani et al., 2019a; Dehghani et al., 2019b); Sathiyanathan et al., 2005; Loto and Oghenerukewe, 2016; Mohanan and Palaniswamy, 2005; Saratha et al., 2009; Philip et al., 2016). This research focusses on the corrosion inhibition and adsorption properties of citrus sinensis (Jafri and Ali, 1976) on carbon steel in dilute HCl and H_2SO_4 solution to assess their corrosion inhibition

* Corresponding author.
E-mail address: tolu.loto@gmail.com (R.T. Loto).

https://doi.org/10.1016/j.sajce.2020.08.004
Received 20 March 2020; Received in revised form 22 August 2020; Accepted 27 August 2020
Available online 30 August 2020

Table 1
Elemental composition (wt.%) of PCS.

Element	C	Si	Mn	P	S	Cu	Ni	Al	Fe
Composition	0.40%	0.17%	0.44%	0.01%	0.01%	0.08%	0.01%	0.03%	Balance

Table 2
Wt. loss data for PCS corrosion in 0.5 M H_2SO_4 and 0.5 M HCl solution at specific CS concentration.

H_2SO_4 PCS Samples	Weight Loss (g)	CS Concentration (%)	Corrosion Rate (mm/y)	CS Inhibition Efficiency (%)
A	4.793	0	15.55	0
B	4.360	2	14.15	9.04
C	3.741	4	12.14	21.95
D	1.864	6	6.05	61.11
E	1.505	8	4.88	68.59
F	1.032	10	3.35	78.47
HCl				
A	2.785	0	9.04	0
B	1.380	2	4.48	50.47
C	1.329	4	4.31	52.28
D	0.555	6	1.80	80.07
E	0.512	8	1.66	81.61
F	0.401	10	1.30	85.61

potential, adsorption properties and concentration for optimum performance.

2. Experimental methods

2.1. Material

Plain carbon steel (PCS) obtained in Lagos, Nigeria has a cylindrical shape with diameter of 0.6 cm. The elemental composition of the steel was determined at the Materials Characterization Laboratory, Department of Mechanical Engineering, Covenant University, Ota, Ogun State, Nigeria as shown in Table 1. PCS was cut into 6 separate test samples with mean length at 0.6 cm. Citrus sinensis (Jafri and Ali, 1976) abbreviated as CS essential oil extracts obtained from NOW Foods, USA have molar mass of 2351.6 g/cm^3. The oil extracts were formulated in volumetric concentrations of 1%, 2%, 3%, 4% and 5% CS in 0.5 M H_2SO_4 (98% analar grade) and 0.5 M HCl solution (37% analar grade).

2.2. Electrochemical tests

Weight loss analysis was performed by total immersion of PCS samples in CS-acid solution at predetermined CS concentrations. The weight of PCS samples was determined at 24 h interval for a total of 480 h. Corrosion rate (C_R) was calculated as follows;

$$C_R = \left[\frac{87.6M}{DAT}\right] \quad (1)$$

M (mg) indicates weight loss, A (cm^2) indicates PCS surface area and T (h) indicates exposure time. Inhibition efficiency (η),% was determined from the equation below;

$$D = \left[\frac{M_1 - M_2}{W_1}\right] \times 100 \quad (2)$$

M_1 and M_2 represent weight loss with and without predetermined concentrations of CS. Potentiodynamic polarization test was performed with the aid of triple electrode set which consists of Pt counter electrode, PCS sample electrode and Ag/AgCl reference electrode within a glass container filled with the CS-acid solution and linked to Digi-Ivy potentiostat. PCS sample electrodes was encased in pre-hardened resin mounts with visible surface area of 1.13 cm^2 for the steel. PCS underwent metallographic preparation with SiC abrasive papers (80, 120, 220,800 and 1000 grits) and 6 μm diamond liquid solution. The potentiostat linked with computer for real-time monitoring was observed from −1.5 V to +1.5 mV at sweep rate of 0.0015 V/s Corrosion current density (J_{CD}) and corrosion potential (E_{CP}) were computed from the Tafel plots. Corrosion rate ($_R$) was determined a shown below;

$$C_R = 0.00327 \times J_{CD} \times Q_{WT}/D \quad (3)$$

Where D (g/cm^3) indicates density and Q_{WT} (g) indicates PCS equivalent weight. Inhibition efficiency (ŋ) was calculated from the relationship below;

$$\eta = 1 - \left[\frac{R_2}{R_1}\right] \times 100 \quad (4)$$

R_1 and R_2 represents corrosion rate with and without CS additions. Optical macroscopic images of PCS surface before and after corrosion test with the use of Omax trinocular metallurgical microscope.

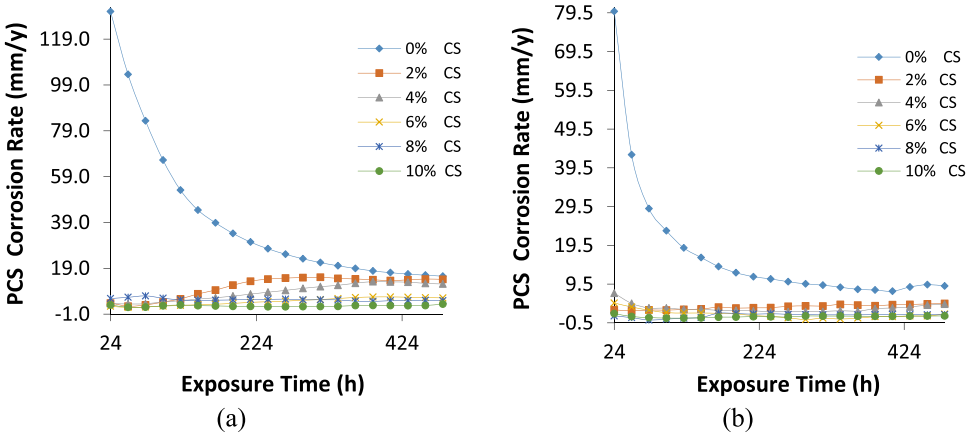

Fig. 1. Plot of PCS corrosion rate versus exposure time at specific CS concentration (a) in H_2SO_4 solution and (b) in HCl solution.

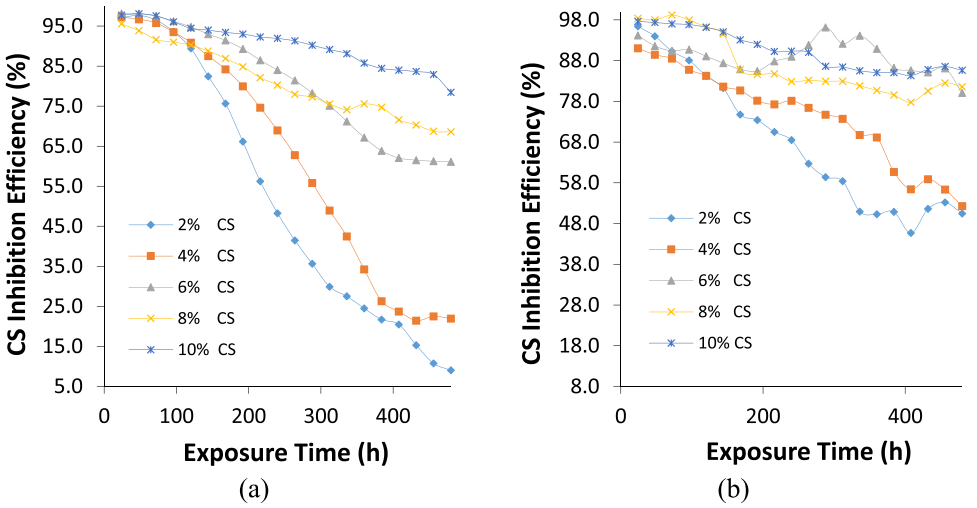

Fig. 2. Plot of CS inhibition efficiency versus exposure time at specific CS concentration (a) in H_2SO_4 solution and (b) in HCl solution.

3. Results and discussion

3.1. Weight loss measurement

Plots of PCS corrosion rate versus exposure time and CS inhibition efficiency versus exposure time at specific CS concentration are shown from Fig. 1(a) to 2(b). Fig. 3(a) to 4(b) shows the optical images (mag. x20) of PCS after corrosion in H_2SO_4 and HCl without CS, after corrosion in both acids at optimal CS concentration (10% CS). The plots of PCS corrosion rate versus exposure time [Fig. 1(a) and (b)] at 0% CS concentration significantly differs from the plots at specific CS concentration due to the electrochemical action of SO_4^{2-} and Cl^- anions with respect to the equations below;

$$Fe(s) + H_2SO_4(aq) \rightarrow FeSO_4(aq) + H_2(g) \quad (5)$$

$$Fe+2HCl(aq) \rightarrow FeCl_2(aq) + H_2 \quad (6)$$

The corrosion reaction mechanism results in surface severe oxidation of PCS and accelerated corrosion as shown in the optical images in Fig. 3(a) and (b) where the degree of PCS surface deterioration from H_2SO_4 solution is much higher. The corrosion rate of PCS in H_2SO_4 and HCl solution initiated at 131.07 mm/y and 79.90 mm/y (24 h) with respect to the equations below. Significant decrease in PCS corrosion rate value (in both acids) with respect to exposure time is due to weakening of the static acid electrolytes with discharged corrosion products. As a result, the corrosion rate of PCS at 0% CS culminated at 15.5 mm/y and 9.04 mm/y in both acids. CS at 2% and 4% concentration in H_2SO_4 solution were significantly insufficient to inhibit the corrosion of PCS as shown in the final corrosion rate values of 14.15 mm/y and 12.14 mm/y. Observation of the plot on Fig. 1(a) shows significant increase in corrosion rate at these concentrations with respect to exposure time. At 6% CS concentration significant decrease in corrosion rate occurred culminating at 6.05% (480 h). At 10% CS concentration, final corrosion rate value of 3.35 mm/y was attained signifying effective corrosion inhibition. In HCl solution, optimal corrosion rate value of PCS decreased from 9.04 mm/y at 0% CS concentration to 4.48 mm/y. CS concentration from 6% to 10% significantly decreased the corrosion rate of PCS culminating at 1.80 mm/y, 1.66 mm/y and 1.30 mm/y.

Observation of the plots of CS inhibition efficiency versus exposure time in both acid solutions shows CS compound performed more effectively in HCl solution compared to H_2SO_4. At 480 h of exposure, inhibition efficiency of CS in H_2SO_4 solution at 2% and 4% CS concentration are 9.04% and 21.95%. These values are significantly below the threshold values for effective corrosion inhibition. The corresponding values in HCl solution are 50.47% and 52.28%. However, significant inhibition value in H_2SO_4 occurred from 6% CS concentration (61.11%). At 5% CS concentration the highest value of 78.47% was attained at 480 h of exposure with the corresponding image shown in Fig. 4(a). The corresponding inhibition values obtained in HCl solution (6% to 10% CS concentration) were significantly higher than the values obtained in H_2SO_4 solution. The values ranged from 80.07% to 85.61%. Fig. 4(b) shows the corresponding image for PCS inhibition at 10% CS concentration. General observation shows CS at most concentration in H_2SO_4 and HCl solution decreases with exposure time, though the rate

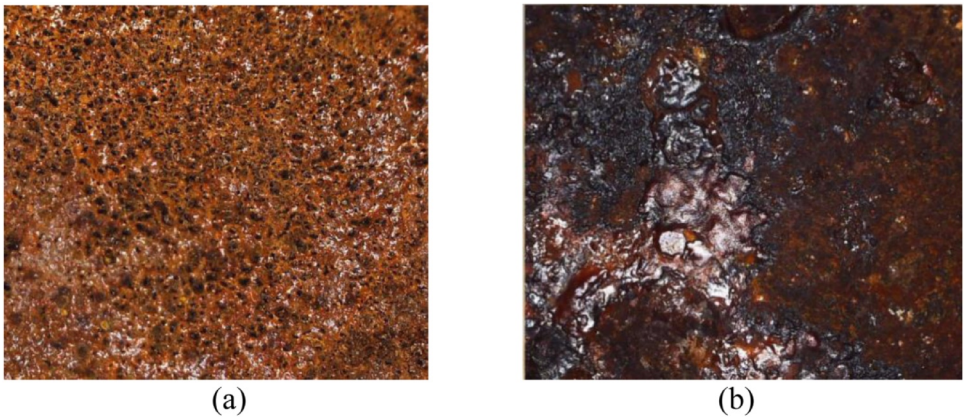

Fig. 3. Optical image of PCS after corrosion in (a) H_2SO_4 solution and (b) HCl solution.

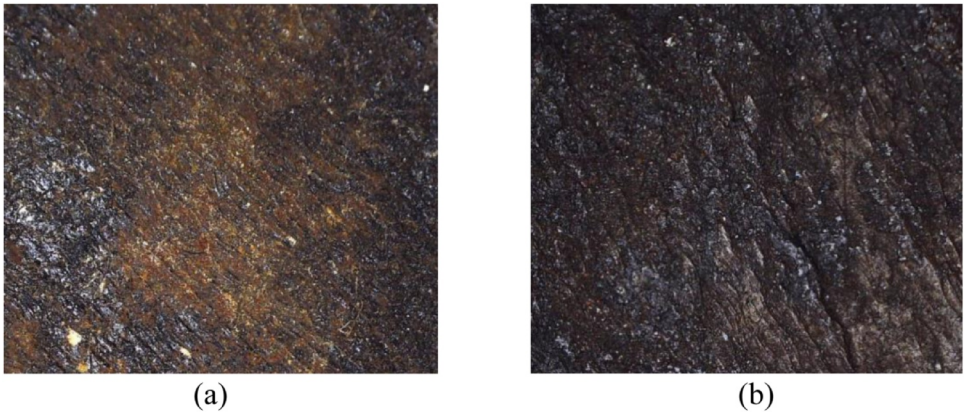

Fig. 4. Optical image of PCS after corrosion at specific CS concentration in (a) H_2SO_4 solution and (b) HCl solution.

of decrease declines with increase in Cs concentration. At 8% and 10% CS concentration the rate of decrease is minimal till around 192 h to 216 h where the progressive increase and relative stability was observed.

3.2. Potentiodynamic polarization studies

Potentiodynamic polarization plots of PCS corrosion in H_2SO_4 and HCl solution at specific CS concentration are shown in Fig. 5(a) and (b). Data obtained from the test is shown in Table 3. Observation of the data shows significant difference between inhibited and non-inhibited PCS in the acid solutions for reasons earlier discussed at the weight loss measurement section. At 0% CS, the corrosion rate of PCS in both acids are 9.47 mm/y and 5.52 mm/y corresponding to corrosion current density of 8.30×10^{-4} A/cm^2 and 4.84×10^{-4} A/cm^2. Decrease in corrosion rate was relatively gradual in H_2SO_4 compared to HCl with effective CS corrosion inhibition on PCS, beginning at 6% CS concentration in H_2SO_4 (62.82%) and 4% concentration in HCl (60.41%). Optimal inhibition efficiency was attained at 10% CS concentration in both acids at 76.93% and 94.90% which corresponds to corrosion rate

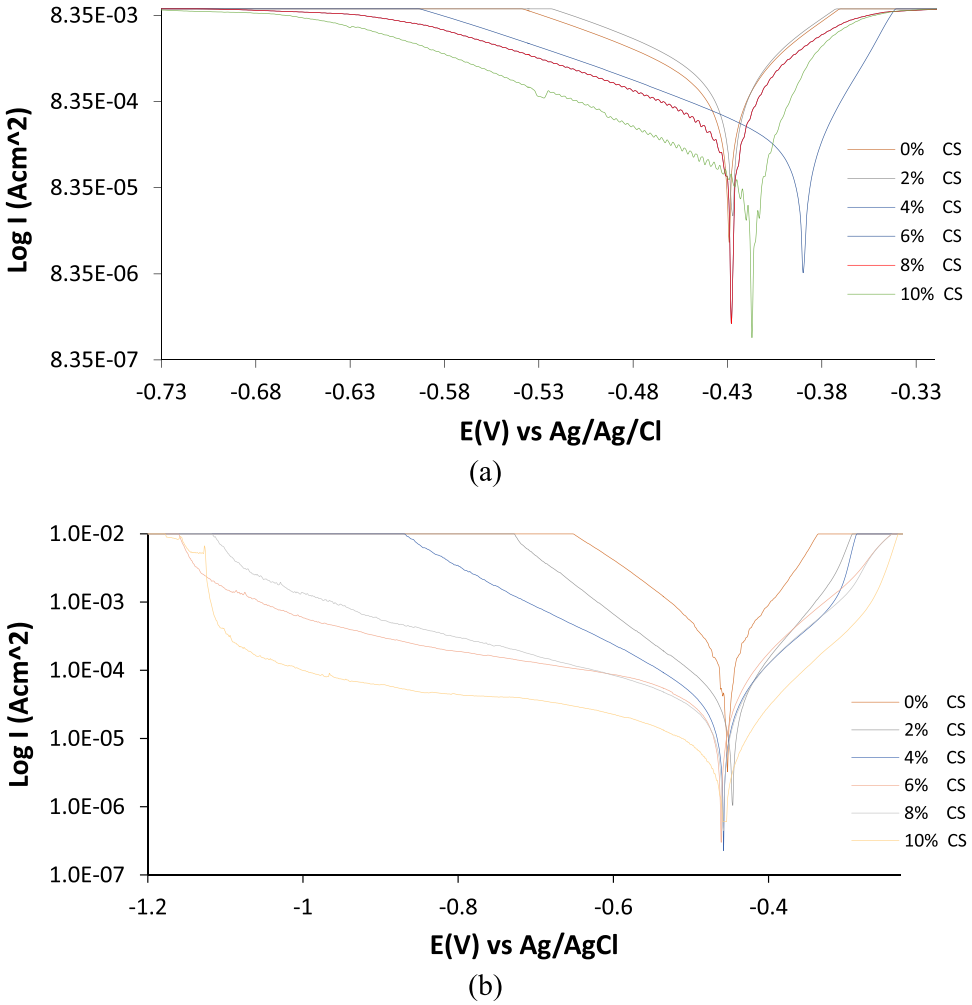

Fig. 5. Potentiodynamic polarization plots PCS corrosion at specific CS concentration in (a) H_2SO_4 solution and (b) in HCl solution.

Table 3
Data for potentiodynamic polarization of PCS in 0.5 M H_2SO_4 and HCl solution at specific CS concentration.

H_2SO_4 Solution Sample	CS Conc. (%)	PCS C_R (mm/y)	CS ξ_F (%)	C_I (A)	C_J (A/cm^2)	C_P (V)	R_p (Ω)	B_c (V/dec)	B_a (V/dec)
A	0	9.47	0	9.38E-04	8.30E-04	−0.429	17.40	−7.203	1.451
B	2	7.58	19.95	7.51E-04	6.64E-04	−0.427	29.49	−7.503	0.138
C	4	6.12	35.35	6.06E-04	5.36E-04	−0.428	43.26	−10.480	2.969
D	6	3.52	62.82	3.49E-04	3.08E-04	−0.390	75.64	−7.943	1.054
E	8	2.84	69.97	2.82E-04	2.49E-04	−0.402	91.24	−2.475	4.046
F	10	2.18	76.93	2.16E-04	1.91E-04	−0.420	118.80	−6.364	9.240
HCl Solution									
Sample	**CS Conc. (%)**	**PCS C_R (mm/y)**	**CS ξ_F (%)**	**C_I (A)**	**C_J (A/cm^2)**	**C_P (V)**	**R_p (Ω)**	**B_c (V/dec)**	**B_a (V/dec)**
A	0	5.52	0	5.47E-04	4.84E-04	−0.453	47.18	−6.646	13.15
B	2	2.76	49.92	2.74E-04	2.42E-04	−0.445	61.19	−5.807	−0.064
C	4	2.19	60.41	2.16E-04	1.92E-04	−0.458	83.81	−5.140	4.930
D	6	0.34	93.83	3.37E-05	2.99E-05	−0.461	761.40	−7.394	10.500
E	8	0.34	93.86	3.35E-05	2.97E-05	−0.458	766.00	−5.107	11.180
F	10	0.28	94.90	2.79E-05	2.47E-05	−0.458	820.80	−5.130	10.730

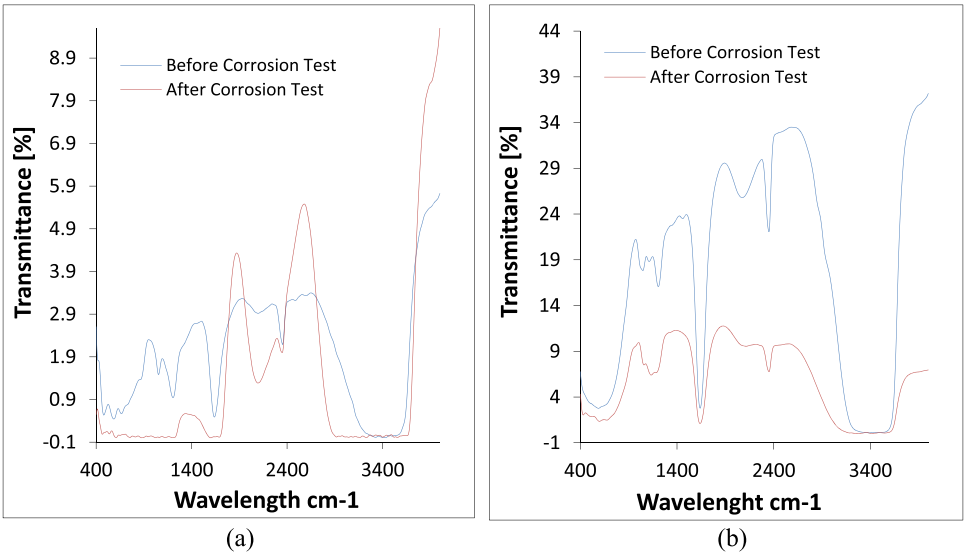

Fig. 6. FTIR spectra of CS/acid solution before and after corrosion test from (a) H_2SO_4 solution and (b) HCl solution.

Table 4
FTIR data of the spectral wavelengths, transmittance, functional groups and molecular bonds from CS-PCS interaction before and after corrosion in H_2SO_4 and HCl solution.

	H_2SO_4	HCl
Before corrosion	572 (*0.470*), 652 (*0.598*), 860 (*1.634*), 1066 (*1.596*), 1192 (*0.995*), 2114 (*2.936*), 2362 (*2.313*) and 3174 – 3602 (*0.274 −0.1983*)	576 (*2.797*), 1040 (*17.871*), 1098 (*19.013*), 1194 (*16.464*), 1654 (*3.542*), 2060 (*25.841*), 2348 (*22.138*), 3204–3610 (*0.839–0.839*)
After corrosion	515–1208 (*0.011*), 1576–1684 (*0.037–0.018*), 2110 (*1.299*), 2336 (*2.029*), 2932–3644 (*0.038–0.053*)	592 (*1.349*), 678 (*1.468*), 1074 (*7.626*), 1240 (*6.448*), 1184 (*6.651*), 1624 (*1.398*), 2340 (*6.972*), 3130–3610 (*0.237–0.237*)
Functional groups	alkyl halides, alkynes, primary, secondary amines, aromatics, aliphatic amines, alcohols, carboxylic acids, esters, ethers, alkynes, nitriles,	alkyl halides, aliphatic amines, alcohols, carboxylic acids, esters, ethers, alkenes, free hydroxyl, H–bonded, alcohols, phenols, alkynes (terminal), primary, secondary amines, amid
Bonds	=*C*–H bend, O–H bend, C–Cl stretch, C–H rock, –C(triple bond)C–H: C–H bend, C–Br stretch, –C(triple bond)C–H: C–H bend, N–H wag, C–H "oop", C–N stretch, C–O stretch, C–H wag (–CH2X), –C(triple bond)C– stretch, C(triple bond)N stretch, O–H stretch, H–bonded, N–H stretch, O–H stretch, C–H stretch, =*C*–H stretch	C–Br stretch, C–N stretch, C–O stretch, C–H wag (–CH2X), –*C* = *C*– stretch, O–H stretch, N–H stretch, –C(triple bond)C–H: C–H stretch

of 2.18 mm/y and 0.28 mm/y, and corrosion current density of 1.91×10^{-4} A/cm^2 and 2.47×10^{-5} A/cm^2. The maximum corrosion potential difference between the value at 0% CS concentration and the value with the highest anodic potential shift (39 mV in H_2SO_4 and 8 mV in HCl) shows CS in both acids is a mixed type inhibitor with strong influence on the anodic and cathodic portion of the polarization plot. Observation of the plots in Fig. 5(a) and (b) shows significant variation in the slopes of the anodic-cathodic portions of the polarization plots with respect to CS concentration. On Fig. 5(a), the steep displacement of anodic-cathodic polarization plots for the carbon steel at 0% and 1% CS concentration is nearly similar due to poor corrosion inhibition as shown in the inhibition efficiency results in Table 3. Increase in CS concentration results in minor decrease in displacement resulting in partial increase in inhibition efficiency. This phenomenon is more pronounced in Fig 5(b) where variation in CS concentration results in significant decrease in slopes of the anodic-cathodic polarization plots,

hence increase in inhibition efficiency compared to the data obtained from H_2SO_4 solution. This is due to the suppression of the oxidation of PCS through surface coverage as proven from the decrease in PCS corrosion rate with increase in CS concentration. Protonated molecules of CS adsorbed unto the ionized steel surface stifling further redox electrochemical processes responsible for corrosion. However, this is less effective in H_2SO_4 solution. Secondly, cathodic reduction reactions involving H_2 evolution and O_2 reduction reactions were also altered by the presence of CS compound. This is more prevalent on the cathodic polarization plot at 6% − 10% CS concentration in HCl and 10% CS concentration in H_2SO_4 solution. The plot in HCl depict pseudo passivation behavior with respect to Cs concentration due to significant decrease in corrosion current density in the presence of CS. This phenomenon is influenced by CS concentration.

3.3. ATF-FTIR spectroscopy analysis

Identification and validation of functional groups and molecular bonds active within cationic inhibitor molecules of CS and responsible for its inhibition behavior and adsorption on PCS surface within the acid media was performed by ATF-FTIR spectroscopy with the results correlated with the conventional ATF-FTIR spectroscopic Table (Socrates, 2004). FTIR spectra of CS/ H_2SO_4 and CS/HCl solutions prior to and immediately after the corrosion test are presented in Fig. 6(a) and 6(b). The FTIR spectra peaks in both Figures shows significant decrease in the peaks transmittance after corrosion at specific wavelengths due to aggregation and adsorption of the functional groups present within CS molecules on PCS surface. Multiple miniature peaks also appeared on Fig. 6(a). The results from corrosion thermodynamics shows the aggregation is due to weak Vander Waals attractive forces which do not necessarily reacts with the steel surface. The decreased transmittance in Fig. 6(b) is due to chemical reaction and chemisorption adsorption of CS functional groups on PCS surface in HCl solution. Table 4 shows the spectra peaks data before and after corrosion, the identified functional groups and molecular bonds. The table shows more functional groups were present on the spectra plots in H_2SO_4 solution compared to HCl due to the higher dissociation constant of H_2SO_4 capable of causing the release/formation of cationic species from the inhibitor molecules. After corrosion, the transmittance (in bracket, Table 4) of the functional groups in both acids generally decreased signifying adsorption.

4. Conclusion

Citrus sinensis essential oil extract effectively inhibited the corrosion of plain carbon steel in H_2SO_4 and HCl solution with inhibition performance subject to variation in the extract concentration. The extract performed more effectively in HCl compared to H_2SO_4 solution. Citrus sinensis was observed to influence the anodic-cathodic reaction processes. However, its inhibition effect shifted more to cathodic inhibition at higher extract concentration in HCl solution. The extract chemisorbed onto the steel in HCl solution while results showed it exhibited physisorption adsorption mechanism in H_2SO_4 solution

Credit author statement

Ekene Henry Mbah and Jennifer Iruoma Ugada are responsible for conducting the research (laboratory work) collation of data, data analysis and manuscript preparation. Roland Tolulope Loto is responsible for the overall supervision of the research, interpretation of the data and discussion of results.

Declaration of Competing Interest

Author's declare no conflict of interest

Acknowledgement

The authors appreciate Covenant University for their support to this research and provision of facilities

References

Ahmad, Z., 2006. Selection of materials for corrosive environment, in Principles of Corrosion Engineering and Corrosion Control. Elsevier Ltd. https://doi.org/10.1016/B978-0-7506-5924-6.X5000-4.

Ashassi-Sorkhabi, H., Masoumi, B., Ejbari, P.E., 2009. Corrosion inhibition of mild steel in acidic media by basic yellow 13 dye. J. Appl. Electrochem. 39 (9), 1497–1501.

Bahlakeh, G., Ramezanzadeh, M., Ramezanzadeh, B., 2017. Experimental and theoretical studies of the synergistic inhibition effects between the plant leaves extract (PLE) and zinc salt (ZS) in corrosion control of carbon steel in chloride solution. J. Mol. 248, 854–870.

Socrates, G., 2004. Infrared and Raman Characteristic Group Frequencies: Tables and Charts. John Wiley & Sons, New Jersey, pp. 18.

Collins, W.D., Weyers, R.E., Al-Qadi, I.L., 1993. Chemical treatment of corroding steel reinforcement after removal of chloride-contaminated concrete NACE Corrosion 49(1) 74–88.

Dariva, G.C., Alexandre, A.F., 2014. Corrosion inhibitors – principles, mechanisms and applications, Developments in Corrosion Protection, Intechopen, pp. 365–379. 10.5772/57255.

Dehghani, A., Bahlakeh, G., Ramezanzadeh, B., Ramezanzadeh, M., 2019a. Electronic/atomic level fundamental theoretical evaluations combined with electrochemical/surface examinations of Tamarindus indiaca aqueous extract as a new green inhibitor for mild steel in acidic solution (HCl 1 M). J. Taiwan Inst. Chem. E. 102, 349–377.

Dehghani, A., Bahlakeh, G., Ramezanzadeh, G., 2019b. Green Eucalyptus leaf extract: a potent source of bio-active corrosion inhibitors for mild steel. Bioelectrochemistry 130, 107339.

Dehghani, A., Poshtiban, F., Bahlakeh, G., Ramezanzadeh, B., 2020. Fabrication of metal-organic based complex film based on three-valent samarium ions-[bis (phosphono-methyl) amino] methylphosphonic acid (ATMP) for effective corrosion inhibition of mild steel in simulated seawater. Constr. Build. Mater. 239, 117812.

Ekpe, U.J., Ibok, U.J., Ita, B.I., Offiong, O.E., Ebenso, E.E., 1995. Inhibitory action of methyl and phenyl thiosemicarbazone derivatives on the corrosion of mild steel in hydrochloric acid. Mater. Chem. Phys. 40, 87–93.

Kuznetsov, Y.I., 1996. Organic Inhibitors of Corrosion of Metals. Springer, US. https://doi.org/10.1007/978-1-4899-1956-4.

Jafri, S.M.H., Ali, S.I., 1976. 1976 Flora of Libya. Al Faateh University Publiation, Tripoli, Libya.

Liu, G.Q., Zhu, Z.Y., Ke, W., Han, C.I., Zeng, C.L., 2001. Corrosion behavior of stainless steels and nickel-based alloys in acetic acid solutions containing bromide ions NACE Corrosion 57(8), 730–38.

Loto, R.T., Loto, C.A., 2012. Effect of P-phenylediamine on the corrosion of austenitic stainless steel type 304 in hydrochloric acid. Int. J. Elect. Sci. 7 (10), 9423–9440.

Loto, C.A., Loto, R.T., 2013. Effect of dextrin and thiourea additives on the zinc electroplated mild steel in acid chloride solution Int. J. Elect. Sci. 8 (12), 12434–12450.

Loto, R.T., 2017. Study of the synergistic effect of 2-methoxy-4-formylphenol and sodium molybdenum oxide on the corrosion inhibition of 3CR12 ferritic steel in dilute sulphuric acid. Results in Phys 7, 769–776.

Loto, R.T., Leramo, R., Oyebade, B., 2018. Synergistic combination effect of salvia officinalis and lavandula officinalis on the corrosion inhibition of low-carbon steel in the presence of SO_4^{2-} and Cl^- containing aqueous environment. J. Fail. Anal. Prev. 18 (6), 1429–1438.

Mohanan, S., Palaniswamy, N., 2005. Corrosion inhibition of mild steel by ethanolic extracts of Ricinus communis leaves. Indian J. Chem. Technol. 12, 356–360.

Loto, R.T., Oghenerukewe, E., 2016. Inhibition studies of Rosmarinus officinalis on the pitting corrosion resistance 439LL ferritic stainless steel in dilute sulphuric acid. Orient. J. Chem. 32 (5), 2813–2832.

Philip, J.Y.N., Buchweshaija, J., Mwakalesi, A., 2016. Corrosion inhibition of amino pentadecylphenols (APPs) derived from cashew nut shell liquid on mild steel in acidic medium. Mats. Sci. & Appl. 7, 396. https://doi.org/10.4236/msa.2016.78036. (2016).

Ramezanzadeh, M., Sanaei, Z., Bahlakeh, G., Ramezanzadeh, B., 2018. Highly effective inhibition of mild steel corrosion in 3.5% NaCl solution by green Nettle leaves extract and synergistic effect of eco-friendly cerium nitrate additive: experimental, MD simulation and QM investigations. J. Mol. 256, 67–83.

Rivera-Grau, L.M., Casales, M., Regla, I., Ortega-Toledo, D.M., Ascencio-Gutierrez, J.A., Porcayo-Calderon, J., Martinez-Gomez, L., 2013. Effect of organic corrosion inhibitors on the corrosion performance of 1018 carbon steel in 3% NaCl solution. Int. J. Elect. Sci. 8, 2491–2503.

Saratha, R., Kasthuri, N., Thilagavathy, P., 2009. Environment friendly acid corrosion inhibition of mild steel by Ricinus communis leaves. Der Pharma Chem 1 (2), 249–257.

Sathiyanathan, R.A.L., Essa, M.M., Maruthamuthu, S., Selvanayagam, M., Palaniswamy, N., 2005. Inhibitory effect of Ricinus communis (Castor-oil plant) leaf extract on corrosion of mild steel in low chloride medium. J. Indian Chem. Soc. 82 (4), 357–359.

Singh, D.D.N., Singh, T.B., Gaur, B., 1995. The role of metal cations in improving the inhibitive performance of hexamine on the corrosion of steel in hydrochloric acid solution. Corros. Sci. 37 (6), 1005–1019.

Winkler, D.A. 2017 Predicting the performance of organic corrosion inhibitors Metals 7(12) 553. 10.3390/met7120553.